Investigation of Natural Convection Heat Transfer in Converging Channel Flows Using a Specklegram Technique

K. D. Kihm
AssistantProfessor.
Mem. ASME

J. H. Kim
Graduate Research
Assistant.

L. S. Fletcher
Thomas A. Dietz Processor.
Fellow ASME

Department of Mechanical Engineering,
Texas A&M University,
College Station, TX 77843

Natural convection heat transfer characteristics in converging vertical channel flows were studied by nonintrusively measuring the wall temperature gradients using a laser specklegram technique. Local and average heat transfer coefficients were obtained for forty different configurations, including five different inclination angles from the vertical, γ = 0, 15, 30, 45 and 60 deg, with eight different channel exit openings for each inclination angle. Correlations for both local and average Nusselt numbers, Eased on the channel length L, were determined as Junctions of Grashof number, where the local Grashof number, based on the channel len th L, ranged up to 7. l6 x 10^6 and the overall Grashof number varied from 3.58 x 10^6 (y = 60 deg) to 7.16 x 10^6 (γ = 0), depending upon the inclination angle. As the top opening was decreased, both local and average Nusselt numbers deviated from the single inclined plate theory and signifcant reductions in heat transfer resulted. The minimum opening ratio, at which the average Nusselt number started decreasing from that Jor the single plate, was determined as $(b/L)_{min}$ = 0.07, 0.1, 0.3, 0.35, and 0.4 for inclination angles of 0, 15, 30, 45 and 60 deg, respectively. For Ra larger than 10^5, average Nusselt numbers, based on the channel opening b, approached the singleplate limit of the vertical channel flow theory, which was modifed to incorporate the reduced gravity due to the inclination. When Ra* was smaller than 10^5, however, neither the single-plate limit nor the fully developed limit properly described the heat transfer characteristics in the converging channel.*

Introduction

Converging air channels that form a triangular enclosure are commonly used in a wide range of buildings, not only for structural strength but also for enhanced insulation of the airfilled space between a ceiling and a roof. Partial openings at both the top and bottom corners of the enclosure will induce converging air flow because of the natural convection boundary layers growing along the inclined roof surfaces (Fig. 1). These openings will reduce the heat transfer from the inclined roof surfaces to the air inside with increase in the connective heat transfer to the outside air through the thermal boundary layers. This enables the ceiling (the bottom plate) to be effectively insulated against the heat penetration from the inclined roof surfaces. When the top opening is too small, however, the boundary layers on the two inclined surfaces will merge and the heat transfer to the outside air will be significantly reduced. The reduction in heat transfer occurred as result of the retardation of the connective air stream because of the narrowed passages, and the phenomenon can be referred as a "choked" state. If the top opening were completely closed, no connective thermal boundary layers would develop. Instead, stratified fluid layers of different densities would be stacked vertically and the heat transfer would occur predominantly by thermal conduction, which results a significant reduction in heat transfer. The choking condition accompanying a heat transfer reduction must be identified and should be avoided to ensure the optimal cooling of inclined surfaces.

Since the pioneering study of heat convection in vertical parallel channel flow by Elenbaas (1942), a number of early

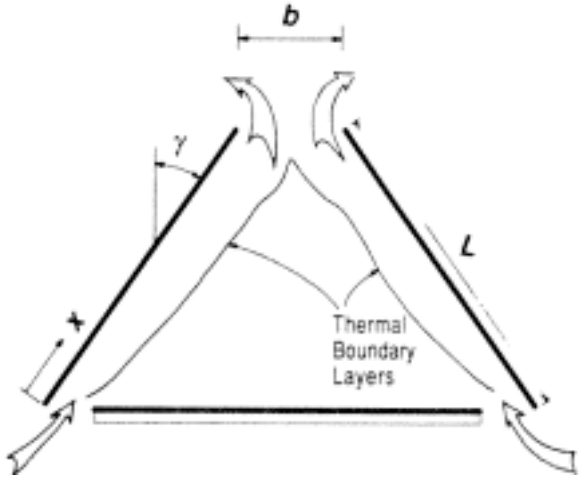

Fig. 1 A schematic illustration of thermal baundary layers in a trlangular enclosure

investigators, e.g., Eckert and Carlson (1961), Levy (1972), Wirtz and Stutzman (1982), Bar-Cohen and Rohsenow (1984), and Anand et al. (1992), have indicated that there exists an optimum plate spacing with the highest average Nusselt number occurring when the natural connective heat transfer along the plates reaches its maximum. Naylor et al. (1991) studied the entrance flow effects numerically using the full elliptic equations with extended inlet boundary conditions. They concluded that a full elliptic solution is necessary to determine accurate local quantities near the channel entrance. Martin et al. (1991) investigated a similar problem numerically, specifically for the case of very low Rayleigh number flows. They found that the well-accepted asymptotic behavior for the fully developed solution was valid only under limited conditions.

Contributed by the Heat Transfer Division and presented at the ASME Winter Annual Meeting, Atlanta, Georgia, December 1-6, 1991. Manuscript received by the Heat Transfer Division December 16, 1991; revision received July 2. 1992. Keywords: Flow Visualization, Natural Convection. Technical Editor: R. Viskanta.

Flack et al. (1979) and Flack (1980) studied heat transfer rates inside a closed triangular enclosure with no openings. The two inclined side walls were heated and cooled, respectively, and the bottom surface was maintained adiabatic. The heat transfer characteristics were seen to be somewhat different from that of a single heated or cooled inclined plate, because of the interference of the thermal boundary layers near the upper corners.

When the upper and lower corners are partially opened, the development of thermal boundary layers will be different and a converging convective flow will result. The heat transfer characteristics, therefore, will be different from the results of the closed system, and also will be different from that of a parallel channel system since the thermal boundary layers develop in a different manner. As a consequence, heat transfer characteristics inside converging channel flow should be investigated because they have not been previously examined.

Heat transfer characteristics in a converging channel configuration, with partial openings on top and bottom corners, were experimentally studied in the present investigation. A nonintrusive specklegram technique (Merzkirch, 1989), with a digital fringe processing system, was employed to measure the wall temperature gradients directly along inclined isothermal surfaces. Both local and average heat transfer coefficients were determined from the measured values of the wall temperature gradients. The effect of the openings on the heat transfer rate was investigated to determine the minimum opening ratio corresponding to the maximum heat transfer from the inclined plates through the convective thermal boundary layers. Differences were identified between the data presented in this paper and data previously obtained for a single inclined plate, and for parallel channel flows formed with double vertical heated plates. The Grashof number was modified to account for the reduced gravitational effect due to the inclination of the isothermal walls, i.e., $Gr_X = Gr_x \cos\gamma$ (Kierkus, 1968; Hasan and Eichhorn, 1979). Local Nusselt numbers are presented in terms of local Grashof numbers. Results for average Nusselt numbers, based on the channel opening *b,* are also presented as function of Ra• as suggested by Elenbaas (1942). The characteristics of the thermal layers were visualized qualitatively using a Schlieren technique.

Experimental Apparatus and Data Processing

The experimental apparatus encompasses the converging channel facility, which provides two inclined isothermal plates and a bottom adiabatic plate, and the support assembly for adjustment of both the inclination angle and the opening ratios. The diagnostic system includes a He-Ne laser specklegram system for direct and nonintrusive measurements of the wall temperature gradients. A computerized evaluation of the specklegram fringe spacings is also briefly described for the data reduction process.

Converging Channel. Each of the two isothermal walls was made with 12.7-mm-thick copper plate with dimensions of 125 mm (L) by 200 mm (H), which was grooved from the balk surface to provide a passage for the circulating water, as shown in Fig. 2. The plate was machined to a 45-deg knife edge on the lower side to reduce the leading edge disturbance on the thermal layer downstream (Yang and Jerger, 1964, and others thereafter). Both plates were heated by a single constant-temperature bath to maintain a uniform wall temperature. A water jacket was installed on the back of each plate using 10-mm thick Lexan. A total of six K-type thermocouple probes were embedded to within 1 mm from the front surface of each plate to monitor the uniformity and consistency of the wall temperature. The typical variance between the readings of the six thermocouples was ±0.2°C for the case of 60°C wall temperature, with a measurement uncertainty of ±0.3 percent. The range of ambient temperature varied from 24.5 to 28°C on a daily basis during the experimental study, and the wall temperature ranged from 56 to 62°C so that the temperature differential, $T_w - T_e$, remained within 32.7 ± 1.2°C throughout the geometric variations. The ambient temperature was also measured with a thermocouple probe and showed negligible variance over a several hour period.

The bottom plate was fabricated from 12.7-mm-thick balsa wood to simulate an adiabatic wall condition. The opening of the two lower corners was adjusted to be one half of the top opening for all the variations of the top opening so that the air inlet and outlet cross-sectional areas were identical. The main role of the bottom adiabatic plate placed herein was to prevent the possible upstream hydrodynamic and/or thermal

Nomenclature

b = opening at the top of the channel
c = distance between the ground glass and the focal plane of a camera (Fig. 3)
c_P = specific heat at constant pressure kJ/kg•°C or J/kg••°C
d = distance between the specklegram slide and the screen (Fig. 4) 4)
Gr_X = local Grashof number ≡ $g\beta \cos(T_w\text{-}T_e)x^3/\nu^2$
GrL = overall Grashof number ≡ $g\beta\cos y(T_W\text{-}T_e)L^3/\nu^2$
g = gravitational constant = 9.8 m/s^2
H = inclined plate dimension parallel to the optical path = 200mm
h = thermal convection coefficient W/m^2•°C
~~h~~ = average thermal convection coefficient, W/m^2•°C
k = thermal conductivity, W/m•°C
L = inclined plate dimension perpendicular to the optical path = 125 mm
m = magnification of a physical object to a speckle image on
m` = magnification of the speckle image to a camera recording image
n = index of refraction of air
Nu_X = local Nusselt number = hxlk
~~Nu_b~~ = average Nusselt number = hb/k
Nu_L = average Nusselt number = hL/k
Ra• = Rayleigh number as defined by Elenbaas (1942)

$$\equiv \frac{g\beta\cos\gamma(T_w - T_e)b^3}{\nu^2}\frac{\nu}{\alpha}\frac{b}{L}$$

s = fringe spacing
T = temperature, °C
x = coordinate parallel to the inclined plate
y = coordinate normal to the inclined plate
z = coordinate parallel to the optical path
β = volumetric coefficient of expansion = $1/T_e$= 1/300 K = 3.333 x 10^{-3}K^{-1}
γ = inclination angle of the inclined plate measured from the vertical, deg
λ = wave length of He-Ne laser = 632.8 nm
μ = dynamic viscosity, kg/m•s
ν = kinematic viscosity of air, m^2/s
ρ = air density, kg/m^3

Subscripts

e = properties evaluated at the ambient temperature
r = properties evaluated at the reference temperature, T_r = T_W - 0.38(T_w - T_e), suggested by Sparrow and Gregg (1958)
w = properties evaluated at the wall temperature of the in clined plate

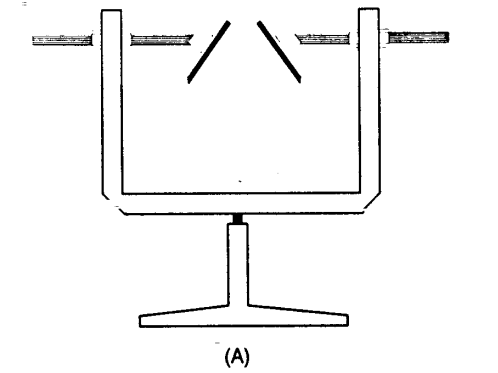

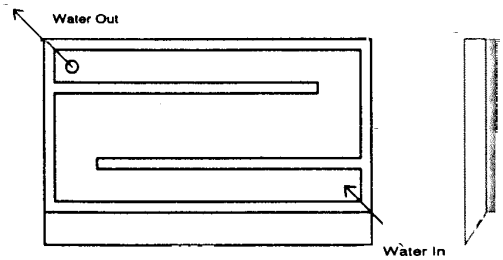

(B)

Fig. 2 Schematic diagrams of the experimental setup: (A) support and positioning assembly, and (B) water jacket for the isothermal Inclined plate

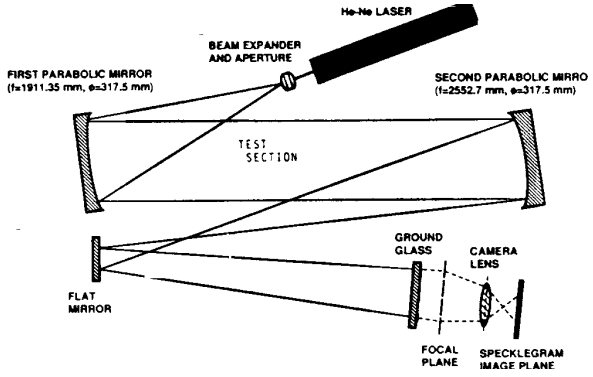

Fig. 3 Optical configuration of the specklegram recording system

fluctuations from entering the channel. Preliminary Schlierer visualization showed that as long as the total inlet area A_i of the two lower corners was kept the same as the upper exit area A_o, the thermal boundary layers near the leading edge of the inclined plate were not affected by the presence of the bottom plate. For the ratio A_i/A_o smaller than unity, the overall hea transfer may decrease since the bottom plate would act to restrict the incoming air flow and also could interfere with the boundary layers near the leading edge of the inclined plate.

A special feature of the support assembly is its versatility it providing a variable spacing between the plates and an ad justable inclination angle for both plates, with 15-deg increments. The end planes of the triangular enclosure were covered with optically flat glass, 3.2 mm thickness, to eliminate, insofar as possible, the three-dimensional ambiguity that otherwise would occur near the ends (Sparrow and Bahrami, 1980; Azevedo and Sparrow, 1985).

Specklegram System. Figure 3 presents the optical layout of the specklegram system that was used to measure the wall

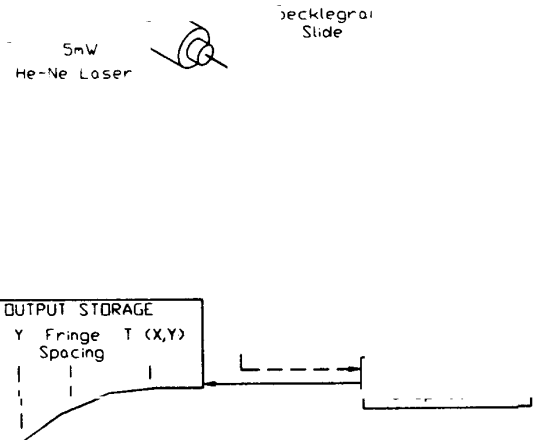

Flg. 4 Schematic Illustration of the data reduction process for speck legram

temperature gradients nonintrusively. A 35 mW He-Ne laser of 632.8 nm wavelength was used as the coherent and monochromatic light source. The laser beam was expanded to 120 mm diameter using a microscope objective lens. The expanded beam was collimated by a parabolic mirror to form parallel light rays throughout the test section. After passing the test section, the light rays were focused by the second parabolic mirror onto a ground glass on which the image of the test section was constructed. Speckles are formed spatially behind the ground glass because of the interference of randomly diffracting rays from the granular surface of the ground glass. Speckles are, therefore, formed regardless of the presence of a test field. When a test field is present in the parallel beam passage, the light rays will be refracted because of the indexof-refraction variations in the test field and the resulting speckles will have different spatial locations with respect to speckles recorded without the test field. Each pair of speckles, with and without the test field, shares the same origination point in the test field.

The specklegram, a superimposed image of speckles with and then without the presence of the test field, was recorded using a 4 by 5 inch format bellows camera with high resolution and medium sensitivity ILFORD pan F50 ASA film. The amount of translocation of individual speckles has a precise relationship to the density or temperature gradient in the test section. A simple consideration of the optical geometry with an assumption of the Gladstone-Dale relationship (Eckert and Goldstein, 1976) derives an expression for the temperature gradient (Kihm et al., 1991):

$$\frac{\partial T}{\partial y} = \frac{\lambda \cdot d}{H \cdot c \cdot s} \cdot \left(\frac{dn}{dT} \right)^{-1} \cdot \frac{m}{m'} \tag{1}$$

where the geometric constants *H, c,* and *d* represent the width of the inclined plate, the distance from the ground glass to the focal plane (Fig. 3), and the distance between the specklegram slide and the screen (Fig. 4), respectively. The magnification of the second parabolic mirror is denoted by m, and m' denotes the magnification of the recording system. The relationship for the refractive index of air at the 632.8 nm wavelength of He-Ne laser gives an expression for the constant, *dnldT* (Vest, 1979):

$$\frac{dn}{dT} = -\frac{1.075 \times 10^{-6}}{(1 + 0.00368T)^2} \tag{2}$$

where T is in degrees Celsius. T was taken as being equal to the wall temperature since the air temperature adjacent to the wall should be closely equal to the wall temperature. The wall temperature variations were negligibly small (± 0.3 percent)

and the measurement uncertainty due to the temperature dependence of *dn/dT is* also expected to be negligibly small.

The temperature gradient, $\partial T/\partial y$, can now be determined from the measurement of the fringe spacing, *s*, of Young's fringes, which are constructed by illuminating the specklegram with a small He-Ne laser (Fig. 4). The fringe spacings were measured using a software called **FRINGE** that scans and identifies locations with the maximum and minimum light intensities on a digitized fringes imaged by a video camera. This digitized measurement of fringe spacing must be very accurate and the measurement uncertainty is estimated to be within ± 1 percent. The constituent equation for the specklegram technique, Eq. (1), should be accurate with ± 1 to 2 percent error at most, since those physical lengths, magnifications, and other optical parameters in the equation were provided from straightforward measurements or from well-established theories.

Additional measurement uncertainties for the wall temperature gradient, $(\partial T/\partial y)_w$, can result from the defocusing of the test section on the specklegram recording plane. The image of the test object on a specklegram must be slightly defocused and this is an essential consequence in recording speckles with a measurable distinctiveness between speckle dislocations. The uncertainty due to the image biasing can be estimated with an image blur ratio (Kihm, 1992), which is defined as a ratio of the defocusing distance measured from the ground glass to the focal length of the Schlieren head, or the second parabolic mirror (Fig. 3). As the measurement location is placed farther away from the optical axis, the uncertainty because of the defocusing will be higher since the light ray diffraction increases with increase in the traverse distance from the optical axis. The maximum uncertainties associated with the image defocusing combined with the measurement location effect were calculated to be within ± 0.3 mm for the case of an object distance of 62.5 mm (equivalent to *L/2)* from the optical axis. In the gray zone, which resulted from the image uncertainties, the signal-to-noise ratios of the data were somewhat reduced, but the fringes were still distinguishable. The speckle dislocation data were obtained at the nearest location to the wall to evaluate wall temperature gradients. The calculations also showed that the maximum value of the image blur ratio was up to 0.8 percent for the worst case. The overall measurement uncertainties for the wall temperature gradient because of the defocusing, therefore, should be within 1 percent for a very conservative estimation.

Data Reduction. Considering an energy balance between an isothermal wall at Tw and the ambient air at temperature T,, the correlation of the local heat transfer coefficient is expressed as:

$$\frac{h(x)}{k} = -\frac{(\partial T/\partial y)_w}{(T_w - T_e)} \tag{3}$$

where the thermal conductivity *k* can be evaYuated at the wall temperature since the heat conduction occurs at the wall. The actual evaluation of the thermal conductivity, however, was not necessary in determining the heat transfer correlations since the local Nusselt number, $Nu_x=h(x)x/k$, was directly determined from the right-hand side of Eq. (3):

$$Nu_x = \frac{h(x)}{k}x = -\frac{(\partial T/\partial y)_w}{(T_w - T_e)}x \tag{4}$$

and the local Grashof number is defined:

$$\mathrm{Gr_x} = g\beta\cos\gamma\,(T_w - T_e)x^3 / \nu_r^2 \tag{5}$$

where the volumetric expansion coefficient for ideal gases

$$\beta = 1/T_e. \tag{6}$$

Assuming that the air density variations were small across the thermal boundary layers for the range of temperatures considered, the reciprocal of the ambient temperature was set equal to β (Holman, 1981). The kinematic viscosity of air, ν_r was obtained at the reference temperature, T_r,

$$T_r = T_w - 0.38(T_w - T_e) \tag{7}$$

This reference temperature, which was suggested for improved fitting by Sparrow and Gregg (1958), results in a slightly higher temperature than the arithmetic mean of the wall and ambient temperatures. If the volumetric expansion coefficient were to be evaluated at the same reference temperature as in Eq. (7), the resultant Grashof number would be reduced by up to 5 percent.

The average convection heat transfer coefficient is then determined by integrating Eq. (3) along the inclined plate length, *L:*

$$\bar{h} = \frac{1}{L}\int_0^L h(x)dx = -\frac{k}{L}\int_0^L \frac{(\partial T/\partial y)_w}{(T_w - T_e)}dx \tag{8}$$

and the average Nusselt number based on the plate length is

$$\overline{Nu_L} = \bar{h}L/k = -\int_0^L \frac{(\partial T/\partial y)}{(T_w - T_e)}dx \tag{9}$$

and the Grashof number based on plate length is

$$Gr_L = g\beta\cos\gamma\,(T_w - T_e)\,L^3 / \nu_r^2 \tag{10}$$

where β and *v,* are specified similarly to the case of the local correlations.

The experimental study of heat transfer using conventional techniques necessitates several requirements since the electric power of the surface (foil) heater is usually measured. The most stringent requirements among these include: (1) the whole experimental apparatus must be extensively insulated to minimize the heat loss through other than the primary surface and (2) the radiation loss from the surface must be subtracted from the measured heater power. The measurement accuracy will be limited because of the heat loss from nonperfect insulation as well as the radiation loss. In determining the heat convection coefficients, both Nu_x and ~~Nu_L~~, using the specklegram technique, neither the radiation heat loss nor the heat loss other than the surface needs to be determined. This is because the specklegram technique exclusively ascertains only the convective heat transfer rate from the surface by directly measuring the wall temperature gradients. The radiation heat transfer from the heated surface is not associated with the measurements and can be considered as a completely separate phenomenon. The bulky insulation material wrapped around the experimental configuration is no longer necessary when the specklegram technique is employed. This simplicity with enhanced accuracy is the primary advantage of the laser specklegram technique and the technique can significantly alleviate the difficulties that would occur in heat transfer experiments with the conventional methods, particularly for the case of natural convection problems where the amount of heat transfer is in general very minute and the heat losses can significantly affect the measurement accuracy.

Results and Discussion

Local and average heat transfer characteristics for converging channel flows along inclined isothermal plates were determined for five different inclination angles, γ=0, 15, 30, 45, and 60 deg from the vertical, and for up to eight different opening ratios, *b/L=0.02,* 0.05, 0.1, *0.2,* 0.3, 0.4, 1, and *2* for each inclination angle. Local and average Nusselt number correlations were determined where overall Grashof number ranged from 3.58 x 10^6 (y = 60 deg) to 7.16 x 10^6 (γ = 0).

Figure 5 presents Young's fringe patterns constructed at different locations on a specklegram taken for y=30 deg and *b/L = 0.2.* The very steep temperature gradient near the inclined wall created distinctive fringes with narrow spacing (inset photos A and B) and the gradual temperature eradient near

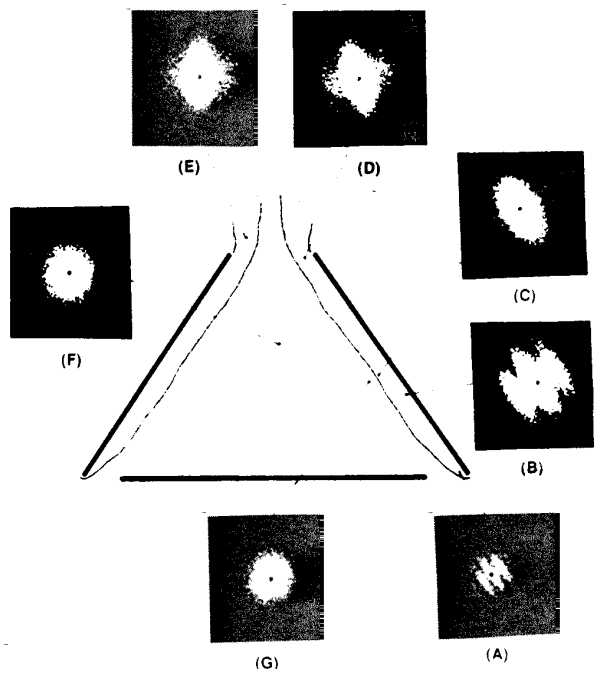

Fig. 5 Locat patterns of the speckle binges in converging flows with inclined isothermal plates

the boundary resulted in less distinctive fringes with wide spacing (inset photo C). At the top opening (inset photos D and E), where thermal boundary layers developed because of the temperature gradient between the heated air from inside and the cooler ambient air, the fringe patterns were observed. Outside the thermal layer (inset photos F and G) no fringe patterns were constructed, indicating zero or extremely low temperature gradients. The fringe orientation, which is perpendicular to a local temperature gradient, indicates the primary direction of heat transfer. The fringe patterns, therefore, provide qualitative information on the temperature gradient as well as the primary direction of heat transfer.

Figure 6 presents the correlations of local heat transfer coefficients for vertical parallel channel flows with several different spacings. The solid line represents the theory of Ostrach (1952) for a vertical isothermal single plate:

$$Nu_X = 0.5046\,(Gr_x/4)^{0.25} \tag{11}$$

Good agreement between the experimental data and the theory was shown for opening ratios down to 0.1, which indicated that each wall acts as an independently inclined plate without affecting each other, when *b/L* was equal to or greater than 0.1. The good agreement also demonstrated the measurement accuracy of the specklegram technique. For *b/L=0.05, the* local Nusselt number started to deviate from the theory when the local Grashof number was larger than 5×10^4. The deviation from the single plate theory implied that the two thermal boundary layers started interfering with each other, which resulted in a decrease in the wall temperature gradients for $Gr_x > 5 \times 10^4$. When the local Grashof number exceeded 10^5, for the case of *b/L=0.05,* the fringes were not clearly constructed since the fully developed thermal boundary layers resulted in horizontally uniform temperature field and the overall heat transfer rate was further decreased. The speckle dislocations were very small and the fringe spacing approached infinity because of the extremely low wall temperature gradients. The minimum opening, at which the thermal layers started interfering with each other and the amount of heat transfer started decreasing from that of a sinrle elate limit, was estimated to be close to *b/L* of 0.05.

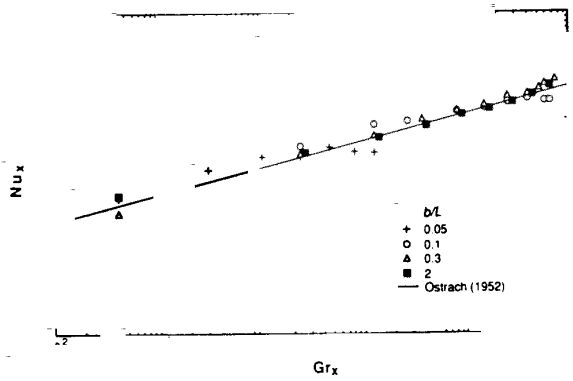

Fig. 6 Local NusseN number versus local Grashof number for a vertical isothermal channel flow

Bar-Cohen and Rohsenow (1984) proposed the following experimentally extrapolated relationship of the minimum opening ratio for the case of a vertical isothermal channel flow:

$$\left(\frac{b}{L}\right)_{\min} = \frac{2.714}{\left(\dfrac{c_p \rho^2 g \beta L^3 (T_w - T_e)}{\mu k}\right)^{1/4}} \tag{12}$$

For the conditions in Fig. 6, $c_P = 1.007$ 1/kg•°C, ρ=1.10564 kg/m^3, g=9.8 m/s, β=3.333×10^{-3} K^{-1}, L=0.125 m, T_w–T_e =32°C, μ= 1.9377×10^{-5} kg/m•s, and k=0.02776 W/ m•°C, $(b/L)_{min}$ *was* calculated to be equal to 0.0584. This calculation agrees fairly well with the value of 0.05, which was estimated from the measurement of the local heat transfer coefficient in Fig. 6.

Figure 7 presents Schlieren pictures of thermal boundary layers along the vertical channel for three different opening ratios of *b/L=0.2, 0.*1, and 0.05. Convective thermal boundary layers appear darker on the Schlieren photographs since the light intensity change is proportional to the temperature (or density) gradient, and regions outside the thermal boundary layers are viewed as relatively bright images indicating very low temperature gradients. For *b/L=0.2,* separate thermal boundary layers developed with no interference with each other (Fig. 7A). The bright region between the thermal layers indicated horizontally uniform temperature distributions and the incoming air was induced to flow upward due to the vertically driven buoyancy force, i.e., a so-called chimney effect. When the opening ratio was reduced to 0.1 (Fig. 7B), thermal layers still grew independently and the vertically induced flow region was developed. The distinctiveness of the thermal boundary layers near the top exit was slightly diminished as the thermal layers started interfering with each other. When the opening ratio was further decreased to 0.05 (Fig. 7C), the two layers merged to be fully developed well before the top opening, and a horizontally uniform temperature field occurred thereafter. The developing thermal layers (dark regions) existed only near the entrance where the most of heat transfer occurred, and in the fully developed region thereafter heat transfer rate would be very small with nearly zero values of wall temperature gradients. From the visualization, $(b/L)_{min}$ was also estimated to be approximately equal to *0.05.*

A rough indication of the start of transition from laminar to turbulent flow in a vertical configuration was suggested by Cebeci and Bradshaw (1988) to be in the range of the local Grashof number, based on the plate length L, from *6.25* x 10^{10} to 1.3 x 10^{11}. The transition condition for the air flow developing along a single vertical plate, however, has been studied by several investigators experimentally as well as analytically: Tritton (1962) used a fiber anemometer to survey the region of intermittent turbulence and suggested a critical value of Gr_x=*8.57* x 10^6. Lloyd and Sparrow (1970) employed an electrochemical flow visualization

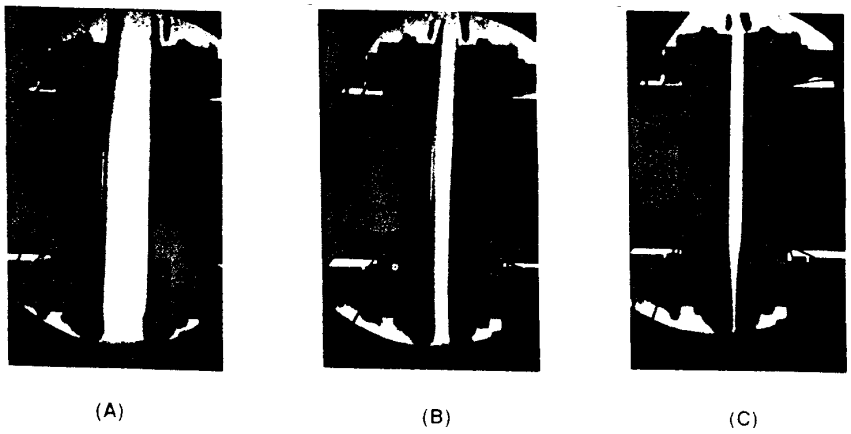

Fig. 7 Schlieren visualization of the development and merging of thermal layers inside the parallel channel with *b/L*=0.2 (A), 0.1 (B), and 0.05 (C)

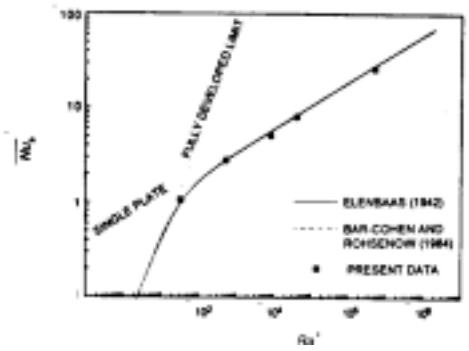

Fig. 8 Average Nusselt number based on the top opening, ~~Nu_b~~ = ~~hb/k~~, versus Rayleigh number, $Ra^* \equiv \frac{g\beta\cos\gamma(T_w-T_e)b^3}{\nu_r^2}\cdot\frac{\nu_r}{\alpha}\cdot\frac{b}{L}$ (Elenbaas, 1942)

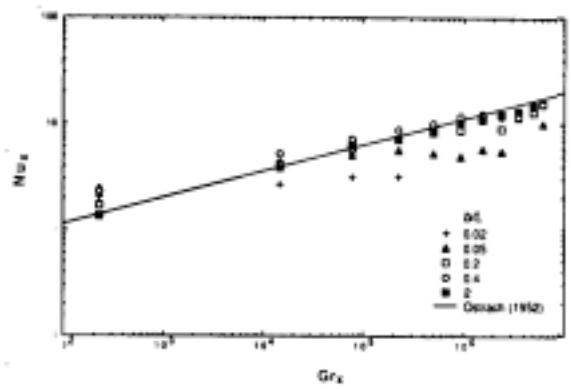

Fig. *9* Local Nusselt number versus local Grashof number for the converging flow with an inclination angle γ =30 deg

technique and determined the onset for fluid disturbances as Gr_X=1.24 x 10^9. Study of theoretical predictions for the critical Grashof number can be further divided into two categories depending on the approaching methods: (1) the traditional wave instability approximation and (2) the vortex instability simulation. Haaland and Sparrow (1973a) studied the problem using a perturbation equation with the wave instability concept and predicted a critical value of Gr_x= 1.17 x 10^6. They also investigated the vortex stability for the natural convection along a vertical plate (Haaland and Sparrow, 1973b). Chen and Tzuoo (1982) made an analysis of vortex instability and their calculation resulted in a value of Gr_X=1.2 x 10^6, very close to that of Haaland and Sparrow (1973a). Tzuoo et al. (1985) later improved the theory by employing the wave instability theory and predicted a somewhat larger value of critical Grashof number, Gr_X=6.2 x 10^6. The Grashof numbers for the present study ranged up to 7.16 x 10^6, which was close to the lower limit of the existing data and predictions. The thermal boundary layers therefore remained stable in most regions along the plate as far as there exist no interferences between the layers, i.e., as long as *b/L* was kept larger than $(b/L)_{min}$.

The local heat convection coefficients were integrated along the plate length following Eq. (8) to determine the average values and the results are presented in Fig. 8. The Nusselt number has been defined based on the channel width, ~~Nu_b~~ ≡ *hb*/k, and the abscissa represents the modified Rayleigh number as defined by Elenbaas (1942):

$$Ra^* = \frac{g\beta\cos\gamma(T_w-T_e)b^3}{\nu_r^2}\frac{\nu_r}{\alpha}\frac{b}{L} \tag{13}$$

where γ is equal to zero for the vertical channel and the subscript *r* denotes an evaluation of the property at the reference temperature given by Sparrow and Gregg (1958). Also presented in Fig. 8 are the experimentally extrapolated correlations for the case of vertical channel flow by Elenbaas (1942) and by Bar-Cohen and Rohsenow (1984). The data showed very good agreement with the previous correlations ensuring the measurement accuracy of the specklegram technique. As discussed earlier with Fig. 6, the data obtained for b/L=0.05 (Ra* ≈ 30) approached the fully developed limit having a lower Nusselt number than the single plate limit because of the merging of thermal layers, which significantly reduces the heat transfer rate. In integrating and averaging the data for the case of b/L=0.05, a logarithmic extrapolation was made for the region of $Gr_X > 10^5$ where the speckle measurements were not available because of overly low wall temperature gradients after the merging of the thermal boundary layers. An interesting thing to note is that a selection of different functional forms for the extrapolation, such as polynomial functions, does not noticeably alter the resultant ~~Nu_b~~ since *h* rapidly decays to zero in the extrapolated region ranging from $Gr_x > 10^5$ to Gr_L =7.16 x 10^6.

Figure 9 presents results of the local Nusselt number versus Grashof number for γ = 30 deg. The solid line again represents Ostrach's theory with a modified Grashof number (Eq. (5)),

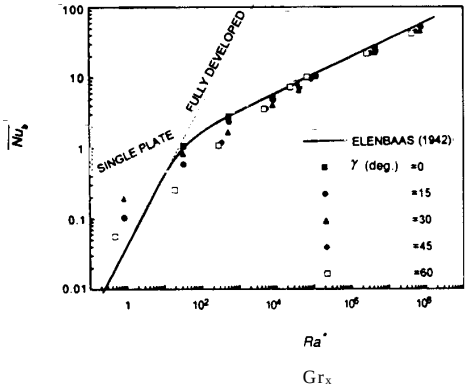

Fig. 10 Local Nusselt number versus local Grashof number for the converging flow with an inclination angle $\gamma = 60$ dog

which accounted for the decreased gravitational effect due to the inclination of the plate. The good agreement of the data for the single inclined plate, represented by the case of $b/L = 2$, with the theory implies that the convective heat transfer along a single inclined plate can be predicted accurately by the mod- if-ied theory by Ostrach (1952). The merging of the thermal boundary layers in the previous vertical channel flow occurred primarily as a result of the growth of the two boundary layers under parallel free-stream air flow. For the case of the inclined isothermal walls, the boundary layers were more unstable and thicker partly because of the reduced buoyancy and partly because of the entrainment of the recirculating flow driven in the converging air flows. When the top opening was large, the flow recirculation disappeared since the converging channel effect was weak, and the thermal layers developed individually without affecting each other. For this case, the heat transfer rate approached that of the inclined single plate results. As the top opening decreased, however, the thermal boundary layers started interfering with each other and the convection heat transfer decreased from the case of the single inclined plate. The Nusselt number variations were nearly flat, indi- cating that the local heat convection coefficient, h, decreased dramatically with x. With decrease in b/L, the discrepancy of the data from the theory started at smaller Grashof number because the merging of thermal boundary layers occurred nearer the leading edge. For the case of b/L of 0.02, the measured Nusselt numbers were below the theory for most regions of the plate except near the entrance and, therefore, the most region of the channel flow must have been fully developed with merged thermal layers. The local Nusselt number showed a slight increase near the top opening after relatively flat values in the merging region. At the top opening, the thermal layers redeveloped and the heat transfer was enhanced gradually because of the heat transfer between the emerging flow stream and the cooler ambient air above.

As the inclination angle, γ, was increased from 30 to 60 deg, the discrepancies between the data and the single plate theory have been increased (Fig. 10). The data measured for a single plate, $b/L = 2$, agreed fairly well with theory, demonstrating that the thermal boundary layer development along the inclined plate with large b/L was similar to the case of the single plate. As the top opening was decreased, however, the thermal boundary layer development was different. The Schlieren visualization indicated that the thermal layers started merging as early as at $b/L = 0.4$. When the inclination angle increased from 30 to 60 deg keeping the top opening ratio the same, the convergence of the inclined channel, which was defined as the ratio of the bottom width to the top opening, had been doubled. This stronger restrictions to the air flow resulted that the thermal boundary layers merged for larger value of b/L for $\gamma = 60$

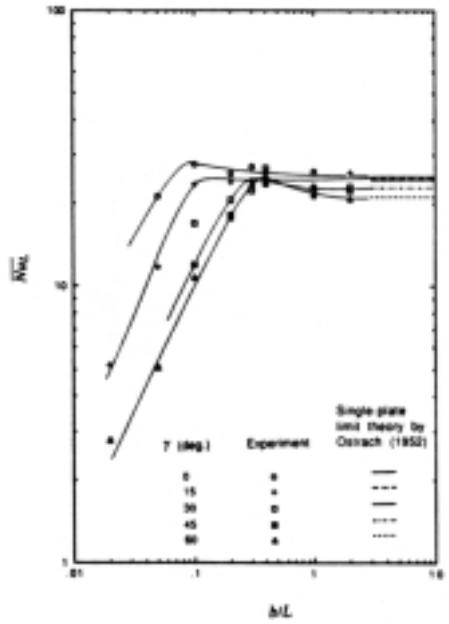

Fig. 11 Average Nusselt number based on the plate length, $\overline{Nu}_L \equiv hL/k$, versus the opening ratio b/L for five different Inclination angles: $\gamma = 0$, 15, 30, 45, and 60 degree[$Gr_L(\equiv g\beta\cos\gamma(T_w - T_E)L^3/\gamma_r^2)$ ranged from 3.58 x 10^6 ($\gamma = 60$ dog) to 7.16 x 10^6 ($\gamma = 0$)]

deg than for the case of $\gamma = 30$ deg. In converging channel flows the flow recirculations act to disturb the thermal layers, whereas the gravitational contribution tends to stabilize the thermal layers. The buoyancy driving of the thermal layers decreased for $\gamma = 60$ deg compared with the case for $\gamma = 30$ deg because of the stronger flow recirculations and the reduced gravity.

Further decrease of the top opening reduced the dependence of the local Nusselt number on the local Grashof number. For b/L values of 0.02 and 0.05, the local Nusselt numbers were (nearly independent of the Grashof number, indicating that the rate of heat transfer dramatically decreased along the inclines plate. For the cases of these extremely narrow top openings the thermal boundary layers were distinctive only near the channel entrance and the two layers merged and mixed thereafter. When the top opening is reduced below $(b/L)_{min}$, the convective heat transfer characteristics for converging channel flows could not be properly described with the theory for a single inclined plate.

Average Nusselt and Grashof numbers were calculated using Eqs. (8)-(10) and are presented for five different inclination angles from 0 to 60 deg as functions of the top opening ratio b/L, in Fig. 11. The overall Grashof number, Gr_L, range from 3.58 x 10^6 ($\gamma = 60$ deg) to 7.16 x 10^6 $\gamma = 0$). When the top opening was large, $\overline{Nu}_L$ approached the single plate limit. Ostrach (1952) regardless of the inclination angles. As b/L decreased, a slight increase in $\overline{Nu}_L$ was observed until the maximum peak was reached. When the top opening decrease further, the average Nusselt number started decreasing an eventually became far smaller than the corresponding singe plate limit. The minimum top opening ratios for the maximum average Nusselt numbers were determined from Fig. 11 and are summarized in Table 1. Table 1 also tabulates the data presented in Fig. 11. The minimum opening ratio increase with increase in the inclination angle with approximately linear relationship.

_Figure 12 presents a rearrangement of the data in terms $\overline{Nu}_L$, versus Ra* and the results are compared with the parallel plate correlations obtained by Elenbaas (1942). For relatively large values of b/L with Ra* larger than 10^5, the average

Table 1 Average Nusselt number, $\overline{Nu}_L = \bar{h}L/k$ for Pr = 0.71; Gr_L ($= g\beta\cos\gamma(T_w-T_e)L^3/\nu_r^2$, ranged from 3.58 x 10^6 (γ= 60 deg) to 7.16 x 10^6 (γ= o)

b/L \ γ(degree)	0	15	30	45	60
0.02	—	5.17	9.72	—	2.78
0.05	21.21	11.799	16.876	—	5.08
0.1	27.867	23.554	16.926	12.06	10.8
0.2	25.65	24.028	20.667	18.187	17.75
0.3	27.122	24.168	22.309	—	23.37
0.4	—	25.816	26.857	23.64	25.25
1.0	26.258	23.35	22.791	22.28	21.53
2.0	—	25.933	23.029	22.44	20.91
∞: single-plate limit (Oseach. 1952)	24.952	24.736	24.07	22.88	20.98
$(b/L)_{min}$	0.07	0.1	0.3	0.35	0.4

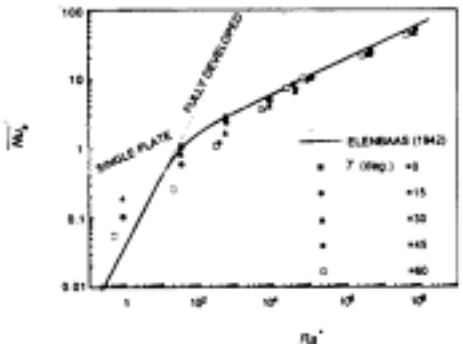

Fig. 12 Average Nusselt number based on the top openlng, $\overline{Nu}_b = \bar{h}b/k$, versus Rayleigh number, Ra* ≡ $\frac{g\beta\cos\gamma(T_w-T_e)b^3}{\nu_r^2}\cdot\frac{\nu_r}{\alpha}\cdot\frac{b}{L}$ (Elenbaas, 1942)

Nusselt number for the converging channel configurations approached the single-plate limit of parallel channel flow. The Rayleigh number was weighted by the factor $\cos\gamma$ to incorporate the reduced gravity due to the plate inclination. As *b/L* decreased for Ra* less than 10^5, however, the data obtained for converging flow agreed neither with the single-plate limit nor with the fully developed limit. The data in general showed lower values of $\overline{Nu}_b$ than those for the case of parallel channel flow. It is believed that the merging of thermal boundary layers nearer the leading edge than for the parallel channel flow primarily contributed to the reduction in heat transfer. The convergence or inclination of the channel plates appeared to induce a premature choking and resulted in a reduction in heat transfer from the case of the vertical channel flows. This observation seemed valid only when Ra* was larger than unity.

For Ra* smaller than unity, the average Nusselt numbers for converging channel flows showed higher values than the fully developed limit of the parallel channel flow. The Schlieren visualization study showed some evidence that when the plates were inclined and have an extremely narrow top opening, *b/L=0.02,* somewhat longer thermal boundary layers developed before they merged or diffused than when the plates were parallel. The overall amount of heat transfer should have been predominantly determined by the region where the thermal boundary layers developed, because after the layers merged or diffused the amount of heat transfer would be significantly diminished. Although it would be necessary to pursue the study for more extensive investigations, it is presently conjectured that the rather higher Nu_b than the fully developed limit for the case of Ra* smaller than unity may be attributed to the apparently longer development of thermal boundary layers along the inclined channel plates than for the case of parallel channel with the same opening at the top.

Summary and Conclusions

Both local and average correlations of heat transfer coefficients have been obtained for laminar natural convection heat transfer occurring inside converging flows. Measurements were made for wall temperature gradients using a nonintrusive specklegram technique for eight different opening ratios ranging from 0.02 to 2 and five different inclination angles from the vertical, down to 60 deg, corresponding to the local Grashof number, Gr_X, ranging up to 7.16 x 10^6 and the average Grashof number, Gr_L, ranging from 3.58 x 10^6 to 7.16 x 10^6 depending on the inclination angle. Results were compared with theoretical predictions for a single isothermal plate by Ostrach (1952) with various inclinations. The data were also rearranged for $\overline{Nu}_b$ versus Ra* and the results were compared with the correlation for vertical channel flows given by Elenbaas (1942).

Conclusions of the present investigation include:

1 The minimum opening ratio has been experimentally determined to be $(b/L)_{min}$ = 0.07, 0.1, 0.3, 0.35, and 0.4 for γ = 0, 15, 30, 45, and 60 deg, respectively.

2 For $b/L < (b/L)_{min}$, the merging of thermal boundary layers for converging channel flows occurs nearer the leading edge than for the case of parallel channel flow and significant reductions in Nu_X and $\overline{Nu}_L$ from the single plate limit result.

3 For $b/L > (b/L)_{min}$, Nu_X and $\overline{Nu}_L$ approaches the theoretical predictions for the single plate limit regardless of the inclination angles as far as the reduced gravity is properly considered.

4 For Ra* larger than 10^5, $\overline{Nu}_b$ approaches the single-plate limit of parallel channel flow regardless of the inclination angles as far as the reduced gravity is properly considered. This, together with conclusion (3), ensures the measurement accuracy of the specklegram technique.

5 For Ra* larger than 1.0, $\overline{Nu}_b$ for the converging channel flows is in general smaller than the case of vertical channel flow even after the reduced gravity was considered. This may be attributed to the fact that the thermal boundary layers merge nearer the leading edge when the heated plates are inclined.

6 For Ra* smaller than 1.0, $\overline{Nu}_b$ exceeds that of the fully developed limit of parallel channel flow. It is believed that this may be due to the longer development of thermal boundary layers along the inclined plates than along the vertical plates.

References

Anand, N. K., Kim, S. H., and Fletcher, L. S., 1992. "The Effect of Plate Spacing on Free Convection Between Heated Parallel Plates," ASME Journal of Heat Transfer, Vol. 114, No. 2, pp. 515-518.

Azevedo, L. F. A., and Sparrow, E. M., 1985, "Natural Convection in Open--Ended Inclined Channels," ASME Journal of Heat Transfer, Vol. 107, pp. 893-901.

Bar-Cohen, A., and Rohsenow, W. M., 1984, "Thermally Optimum Spacing of Vertical, Natural Convettion Cooled, Parallel Plates," ASME Journal of Heat Transfer, Vol. 106, pp. 116-123.

Cebeci, T., and Bradshaw, P., 1988, *Physical and Computational Aspects of Convecrive Hear Transfer,* Springer-Verlag, New York, p. 274.

Chen, T. S., and Tzuoo, K. L., 1982, "Vortex Instability of Free Convection Flow Over Horizontal and Inclined Surfaces," ASME Journla, of Heat Transfer, Vol. 104, pp. 637-643.

Eckert, E. R., and Carlson, W. O., 1961, "Natural Convection in an Air Layer Enclosed Between Two Vertical Plates With Different Temperatures." *lnt. J. Heat Mass Transfer, Vol.* 2, pp. 106-120.

Eckert, E. R. G., and Goldstein, R. J., eds., 1976, *Measurements in Heat Transfer,* McGraw-Hill, New York, pp. 241-244.

Elenbaas, W., 1942, "Heat Dissipation of Parallel Plates by Free Convection." *Physica, Vol.* 9, No. 1, pp. I-28.

Flack, R. D., Konopnicki, T. T., and Rooke, J. H., 1979, "The Measurement

of Natural Convective Heat Transfer in Triangular Enclosures," ASME Journal of Heat Transfer, Vol. 101, pp. 648-654.

Flack, R. D., 1980, "The Experimental Measurement of Natural Convection Heat Transfer in Triangular Enclosures Heated or Cooled From Below ASME Journal of Heat Transfer, Vol. 102, PP- 770-772.

Haaland, S. E., and Sparrow, E. M., 1973a, "Wave Instability of Natural Convection Flow on Inclined Surfaces Accounting for Nonparallelism of the Basic Flow," ASME Journal of Heat Transfer, Vol. 96, pp. 405-407.

Haaland, S. E., and Sparrow, E. M., 1973b, "Vortex Instability of Natural Convection Flow on Inclined Surfaces," *Int. J. Heat Mass Transfer,* Vol. 16, pp. 2355-2367.

Hasan, M. M., and Eichhorn, R., 1979, "Local Nonsimilarity Solution of Free Convection Flow and Heat Transfer From an Inclined Isothermal Plate," ASME Journal of Heat Transfer, Vol. 101, pp. 642-647.

Holman, J. P., 1981, *Heat Transfer,* 5th ed., McGraw-Hill, New York, p. 267.

Kierkus, W. T., 1968, "An Analysis of Laminar Free Convection Flow and Heat Transfer About an Inclined Isothermal Plate," *Int. J. Heat Mass Transfer,* Vol. II, pp. 241-253.

Kihm, K. D., Kastell, D., and Fletcher, L. S., 1991, "Study of Thermal Boundary Layers Occurring Around the Leading Edge of a Vertical Isothermal Wall Using Speckle Photography," *Proceedings ASMEIJSME Thermal Engineering Conference,* J. R. Lloyd and Y. Kurosaki, eds., Vol. 1, pp. 25-33.

Kihm, K. D., 1992, "Image Blurring of Test Section Boundary in a Laser Specklegram Techirique Measuring Temperature Gradients of Compressible Medium," *Applied Optics,* Vol. 31, No. 28, pp. 5907-5910.

Levy, E. K., 1972, "Optimum Plate Spacing for Laminar Natural Convection Heat Transfer From Parallel Vertical Isothermal Flat Plates," ASME Journal of Heat Transfer, Vol. 93, pp. 463-465.

Lloyd, J. R., and Sparrow, E. M., 1970, "On the Instability of Natural Convection Flow on Inclined Plates," *Journal fluid Mechanics,* Vol. 42, pp. 465-470.

Martin, L., Raithby, G. D., and Yovanovich, M. M., 1991, "On the Low Rayleigh Number Asymptote for Natural Convection Through an Isothermal, parallel-plate Channel," , ASME Journal of Heat Transfer, Vol. 113, pp. 899-905.

Merzkirch, W., 1989, "Speckle Photography," in: *Handbook of Flow Visualization,* W. J. Yang, ed., Hemisphere Publishing Corp., New York, Ch. 11.

Naylor, D., Floryan, J. M., and Tarasuk, J. D., 1991, "A Numerical Study of Developing Free Convection Between Isothermal Vertical Plates," ASME Journal of Heat Transfer, Vol. 113, pp. 620-626.

Ostrach, S., 1952, "An Analysis of Laminar Free Convection Heat Transfer About a Flat Plate Parallel to the Direction of the Generating Body Force," NACA TN-2635.

Sparrow, E. M., and Gregg, J. L., 1958, "The Variable Fluid Property Problem of Free Convection," ASME Journal of Heat Transfer, Vol. 80, pp. 879-886.

Sparrow, E. M., and Bahrami, P. A., 1980, "Experiments on Natural Convection From Vertical Parallel Plates With Either Open or Closed Edges," ASME Journal of Heat Transfer, Vol. 102, pp. 221-227.

Sparrow, E. M., and Azevedo, L. F. A., 1985, "Vertical-Channel Natural Convection Spanning Between the Fully-Developed Limit and the Single-Plate Boundary-Layer Limit," *Int. J. Heat Mass Transfer,* Vol. 28, No. 10, pp. 1847-1857.

Trition, D. J., 1962, "Transition to Turbulence in the Free Convection Boundary Layers on an Inclined Heated Plate, *Journal of Fluid meechanics,* Vol. 16, pp. 417-435.

Tzuoo, K. L., Chen, T. S., and Armaly, B. F., 1985, "Wave Instability of Natural Convection Flow on Inclined Surfam," ASME Journal of Heat Transfer, Vol. 107, pp. 107-111.

Vest, C. M., 1979, *Holographic Interferometry,* Wiley, New York, pp. 363 - 365.

Yang, K. T., and Jerger, E. W., 1964, "First-Order Perturbations of Laminar Free-Convection Boundary Layers an a Vertical Plate," ASME Journal of Heat Transfer, Vol. 86, pp. 107-115.

Wirtz, R. A., and Stutzman, R. J., 1982, "Experiments on Free Convection Between Vertical Plates With Symmetric Heating," ASME Journal of Heat Transfer, Vol. 104, pp. 501-507.